

Interaction Note

Note 101

April 1972

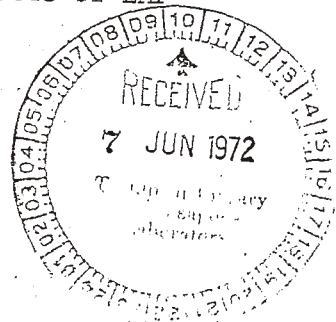
Calculation of the Induced Surface Current Density on a Perfectly Conducting Body of Revolution

M. I. Sancer and A. D. Varvatsis  
Northrop Corporate Laboratories  
Pasadena, California

Abstract

The analysis contained in this note is based on the magnetic-field integral equation simplified to account for the rotational symmetry and perfect conductivity of the scattering body. Detailed calculations are presented which lead to a set of equations upon which a computer code is based. This code can be used to calculate the induced surface current that results when the body is illuminated by a plane wave. As an example, this code is used to calculate the current induced on a finite cylinder when the angle of incidence of a plane wave is varied. Plots of the induced current versus both frequency and time are presented. The frequency plots correspond to the incident plane wave having a time harmonic dependence while the time-domain plots correspond to the incident plane wave having a step-function time dependence.

body of revolution, scattering, surface current, effects of EMP



## I. Introduction

The problem of scattering by a perfectly conducting body of revolution has been studied using the electric field formulation [1]. This formulation is particularly useful when the length of the body is much greater than its width. When this is not the case, an analysis based on the magnetic field integral equation is more appropriate. In this note we start with the magnetic field integral equation for the induced surface current density and specialize its representation to account for the rotational symmetry of the scattering body. We do this by expanding both the incident field and the induced field in an infinite series of trigonometric functions having arguments that are integer multiples of the azimuthal angle,  $\phi$ . We then perform the  $\phi$  integration and obtain an infinite set of decoupled integral equations for the expansion coefficients. These equations are decoupled for each integer multiple of  $\phi$ ; however, there are two expansion coefficients for each integer corresponding to the two orthogonal directions that current can flow on the body and they remain coupled. These expansion coefficients are functions of only one linear dimension, the arc length along the body. Because of this we require only a one dimensional zoning of the body to solve for these coefficients rather than the two dimensional zoning that would be required if we attempted to solve the original integral equation without performing the expansion.

We present detailed calculations which place no significant limitations on the shape of the body other than the rotational symmetry. Our results are in the form of a finite set of linear algebraic equations for each expansion coefficient. This set of equations forms the basis of a computer code that ultimately inverts the matrix associated with these equations. The elements of the matrix are readily calculated from our final equations once the shape of the rotationally symmetric body is specified. Included in the code is the capability of determining the surface current density when the incident plane wave has an arbitrary time dependence. This is accomplished by utilizing the analysis contained in this note and then employing Fourier inversion techniques.

To illustrate that the code is functioning we calculate the total current induced on a perfectly conducting cylinder of finite length when it is illuminated

by a plane wave. We vary the angle of incidence of the plane wave and consider the case where it is time harmonic as well as the case where its time dependence is a step function. This problem is of interest in its own right since missiles are often modeled by finite cylinders. By allowing the angle of incidence to vary we extend the work of a previous note [2]. It should be mentioned that much of the theoretical analysis contained in this note is similar to the work of Carlisle presented in a company report [3].

## II. Formulation of the Integral Equation

The integral equation governing the scattering of a monochromatic electromagnetic plane wave by a perfectly conducting body in free space is well known and has the form

$$\frac{1}{2} \underline{K}(\underline{r}) = \underline{K}^{inc}(\underline{r}) + \int_S \hat{n}(\underline{r}) \times [\nabla G(\underline{r}, \underline{r}') \times \underline{K}(\underline{r}')] dS' \quad (1)$$

where  $\underline{K}$  is the total surface current density on the scattering body,  $\underline{K}^{inc} = \hat{n} \times \underline{H}^{inc}$ ,  $\underline{H}^{inc}$  is the incident magnetic field and  $G(\underline{r}, \underline{r}') = [\exp ik|\underline{r} - \underline{r}'|]/4\pi|\underline{r} - \underline{r}'|$  is the free-space Green's function. Both position vectors  $\underline{r}$  and  $\underline{r}'$  refer to points on the surface of the body. We will cast (1) in a form suitable to the geometry of a body of revolution. To that effect we introduce a local orthogonal curvilinear system as depicted in Fig. 1. The three unit vectors  $\hat{n}$ ,  $\hat{\phi}$ ,  $\hat{t}$  form a right-handed triad and are defined as follows.  $\hat{n}$  points in the direction of the outward normal on the surface,  $\hat{\phi}$  is the usual azimuthal unit vector, and  $\hat{t}$  is tangent to the curve formed by the intersection of the surface of the body and a plane passing through the point of interest and the z axis. The angle between  $\hat{t}$  and  $\hat{z}$  is denoted by  $\nu$  and varies from  $-180^\circ$  to  $180^\circ$  (see Figs. 1a and 1b). The relationships between the local triad  $\hat{n}$ ,  $\hat{\phi}$ ,  $\hat{t}$  and the cartesian triad  $\hat{x}$ ,  $\hat{y}$ ,  $\hat{z}$  are

$$\begin{aligned} \hat{n} &= \cos \nu \cos \phi \hat{x} + \cos \nu \sin \phi \hat{y} - \sin \nu \hat{z} \\ \hat{\phi} &= -\sin \phi \hat{x} + \cos \phi \hat{y} \\ \hat{t} &= \sin \nu \cos \phi \hat{x} + \sin \nu \sin \phi \hat{y} + \cos \nu \hat{z} \end{aligned} \quad (2)$$

In what follows we rewrite (1) in component form in terms of the coordinates of our new local curvilinear system. Referring to (1) we note that

$$\begin{aligned} \hat{t} \cdot [\hat{n} \times (\nabla G \times \underline{K})] &= (\hat{t} \times \hat{n}) \cdot (\nabla G \times \underline{K}) = \hat{\phi} \cdot (\nabla G \times \underline{K}) \\ \hat{\phi} \cdot [\hat{n} \times (\nabla G \times \underline{K})] &= (\hat{\phi} \times \hat{n}) \cdot (\nabla G \times \underline{K}) = -\hat{t} \cdot (\nabla G \times \underline{K}) \end{aligned} \quad (3)$$

and

$$\nabla G \times \underline{K} = \frac{1-ikR}{4\pi R^3} e^{ikR} (\underline{R} \times \underline{K}), \quad \underline{R} = \underline{r}' - \underline{r} \quad (4)$$

Next we write  $\underline{R} \times \underline{K}$  in component form

$$\begin{aligned} \underline{R} \times \underline{K} = & \hat{x} \{ (\rho' \sin \phi' - \rho \sin \phi) \cos v' K_{t'} - (z' - z) (\sin v' \sin \phi' K_{t'} \\ & + \cos \phi' K_{\phi'}) \} + \hat{y} \{ - (\rho' \cos \phi' - \rho \cos \phi) \cos v' K_{t'} \\ & + (z' - z) (\sin v' \cos \phi' K_{t'} - \sin \phi' K_{\phi'}) \} \\ & + \hat{z} \{ (\rho' \cos \phi' - \rho \cos \phi) (\sin v' \sin \phi' K_{t'} + \cos \phi' K_{\phi'}) \\ & - (\rho' \sin \phi' - \rho \sin \phi) (\sin v' \cos \phi' K_{t'} - \sin \phi' K_{\phi'}) \} \end{aligned} \quad (5)$$

Eq. (3) now can be rewritten as

$$\begin{aligned} \hat{t} \cdot [\hat{n} \times (\nabla G \times \underline{K})] \\ = \frac{1-ikR}{4\pi R^3} e^{ikR} \left\{ \left[ [(z' - z) \sin v' - \rho' \cos v'] \cos(\phi' - \phi) + \rho \cos v' \right] K_{t'} \right. \\ \left. - \sin(\phi' - \phi) (z' - z) K_{\phi'} \right\} \end{aligned} \quad (6)$$

$$\begin{aligned} \hat{\phi} \cdot [\hat{n} \times (\nabla G \times \underline{K})] \\ = \frac{1-ikR}{4\pi R^3} e^{ikR} \left\{ \sin(\phi' - \phi) [\rho \sin v' \cos v - \rho' \sin v \cos v' + (z' - z) \sin v \sin v'] K_{t'} \right. \\ \left. + \left[ \cos(\phi' - \phi) [(z' - z) \sin v + \rho \cos v] - \rho' \cos v \right] K_{\phi'} \right\} \end{aligned} \quad (7)$$

Next we expand  $\underline{K}(K_{\phi}, K_t)$  in a Fourier series in the  $\phi$  coordinate. To that effect we first examine the Fourier expansion of the incident current density  $\underline{K}^{inc} = \hat{n} \times \underline{H}^{inc}$

Consider a monochromatic ( $e^{-i\omega t}$ ) plane wave incident upon the axially symmetric conducting body. Without loss of generality we orient the  $xz$  plane so that the  $\underline{k}$  vector has no  $y$  component. The angle between  $\underline{k}$  and  $z$  is denoted by  $\theta_i$  and  $\underline{k}$  has a negative  $x$  component (see Fig. 2). The incident magnetic field forms an angle  $\theta_p$  with the  $y$  axis. We stipulate that if  $\theta_p$  varies between  $0$  and  $180^\circ$  the magnetic field has negative  $x$  and  $z$  components. Assuming that  $\underline{H}^{inc}$  has unit amplitude we can write down the analytical expression for it

$$\underline{H}^{inc} = [(-\hat{x} \cos \theta_i - \hat{z} \sin \theta_i) \sin \theta_p + \hat{y} \cos \theta_p] e^{ik(z \cos \theta_i - x \sin \theta_i)}$$

From Maxwell's equation  $-i\omega \underline{E} = \nabla \times \underline{H}$ , or simple geometrical considerations ( $\underline{E}^{inc}$  has to lie in the plane formed by  $\underline{H}^{inc}$  and the  $y$  axis and  $\underline{k}$ ,  $\underline{E}^{inc}$ ,  $\underline{H}^{inc}$  form a right-handed triad) the expression for  $\underline{E}^{inc}$  is

$$\underline{E}^{inc} = \left(\frac{\mu_0}{\epsilon_0}\right)^{1/2} [(\hat{x} \cos \theta_i + \hat{z} \sin \theta_i) \cos \theta_p + \hat{y} \sin \theta_p] e^{ik(z \cos \theta_i - x \sin \theta_i)}$$

The axis of revolution is  $z$  and for  $\theta_p = 0$  or  $180^\circ$  the electric field lies in the plane  $\hat{k}$ ,  $\hat{z}$  and we then talk about parallel polarization, whereas for  $\theta_p = 90^\circ$  the electric field has a perpendicular polarization. For a general  $\theta_p$  we can decompose the electric field into the two polarizations and the incident current density  $\underline{K}^{inc} = \hat{n} \times \underline{H}^{inc}$  can be decomposed similarly

$$\begin{aligned} \hat{t} \cdot \underline{K}_{||}^{inc} &= \cos \theta_p \cos \phi e^{ik(z \cos \theta_i - x \sin \theta_i)} \\ \hat{\phi} \cdot \underline{K}_{||}^{inc} &= -\cos \theta_p \sin \nu \sin \phi e^{ik(z \cos \theta_i - x \sin \theta_i)} \\ \hat{t} \cdot \underline{K}_{\perp}^{inc} &= \sin \theta_p \cos \theta_i \sin \phi e^{ik(z \cos \theta_i - x \sin \theta_i)} \\ \hat{\phi} \cdot \underline{K}_{\perp}^{inc} &= \sin \theta_p (\cos \nu \sin \theta_i + \sin \nu \cos \theta_i \cos \phi) e^{ik(z \cos \theta_i - x \sin \theta_i)} \end{aligned} \quad (8)$$

Recalling that

$$e^{-ia \cos \phi} = \sum_{m=0}^{\infty} \epsilon_m i^{-m} J_m(a) \cos m\phi, \quad \epsilon_m = 2 \quad m \neq 0, \quad \epsilon_0 = 1$$

we can easily show (by appropriate differentiation) that

$$\begin{aligned} \cos \phi e^{-ia \cos \phi} &= - \sum_{m=0}^{\infty} i^{-(m+1)} J'_m(a) \cos m\phi \\ \sin \phi e^{-ia \cos \phi} &= - \sum_{m=0}^{\infty} m i^{-(m+1)} \frac{J_m(a)}{a} \sin m\phi \end{aligned} \quad (9)$$

Noting that  $x = \rho \cos \phi$  and relating (8) to (9) we understand that the  $\underline{K}^{\text{inc}}$  components can be represented by a pure cosine or sine series with the following results

$$\begin{aligned} (K_{\parallel}^{\text{inc}})_t &= \sum_{m=0}^{\infty} (K_1^{\text{inc}})_{\parallel m} \cos m\phi \\ (K_{\parallel}^{\text{inc}})_\phi &= \sum_{m=0}^{\infty} (K_2^{\text{inc}})_{\parallel m} \sin m\phi \\ (K_{\perp}^{\text{inc}})_t &= \sum_{m=0}^{\infty} (K_1^{\text{inc}})_{\perp m} \sin m\phi \\ (K_{\perp}^{\text{inc}})_\phi &= \sum_{m=0}^{\infty} (K_2^{\text{inc}})_{\perp m} \cos m\phi \end{aligned} \quad (10)$$

$$\begin{aligned} (K_1^{\text{inc}})_{\parallel m} &= - \cos \theta_p J'_m(k\rho \sin \theta_i) \epsilon_m \psi_m \\ (K_2^{\text{inc}})_{\parallel m} &= \cos \theta_p \sin \nu \frac{m J_m(k\rho \sin \theta_i)}{k\rho \sin \theta_i} \epsilon_m \psi_m \\ (K_1^{\text{inc}})_{\perp m} &= - \sin \theta_p \cos \theta_i \frac{m J_m(k\rho \sin \theta_i)}{k\rho \sin \theta_i} \epsilon_m \psi_m \\ (K_2^{\text{inc}})_{\perp m} &= \sin \theta_p [\sin \nu \cos \theta_i J'_m(k\rho \sin \theta_i) - i \cos \nu \sin \theta_i J_m(k\rho \sin \theta_i)] \epsilon_m \psi_m \end{aligned} \quad (11)$$

where  $\psi_m = \exp i[kz \cos \theta_i - (m+1)\pi/2]$ .

In view of Eq. (10) the incident current density can be written as

$$\underline{K}^{inc} = (\underline{K}^{inc})_{\parallel} + (\underline{K}^{inc})_{\perp} = K_t^{inc} \hat{t} + K_{\phi}^{inc} \hat{\phi}$$

and

$$K_t^{inc} = \sum_{m=0}^{\infty} [(K_1^{inc})_{\parallel m} \cos m\phi + (K_1^{inc})_{\perp m} \sin m\phi] \quad (12)$$

$$K_{\phi}^{inc} = \sum_{m=0}^{\infty} [(K_2^{inc})_{\parallel m} \sin m\phi + (K_2^{inc})_{\perp m} \cos m\phi]$$

For simplicity we define

$$(\underline{K}_1^{inc})_{\parallel m} = K_{1m}^{inc}, \quad (\underline{K}_1^{inc})_{\perp m} = K'_{1m} \quad (13)$$

$$(\underline{K}_2^{inc})_{\parallel m} = K_{2m}^{inc}, \quad (\underline{K}_2^{inc})_{\perp m} = -K'_{2m}$$

The reason for the minus sign will become apparent later. In view of (12) and (13) the total current density  $\underline{K}$  will have a Fourier expansion of the form

$$K_t = \sum_{m=0}^{\infty} K_{1m} \cos m\phi + K'_{1m} \sin m\phi \quad (14)$$

$$K_{\phi} = \sum_{m=0}^{\infty} K_{2m} \sin m\phi - K'_{2m} \cos m\phi$$

With the aid of Eq. (6), (7) and (12), (13) and (14), Eq. (1) can be rewritten in component form for the  $m^{\text{th}}$  modes utilizing the orthogonality properties of the trigonometric functions

$$\frac{1}{2} K_{1m}(t) = K_{1m}^{inc}(t) + \int_0^L A_m(t, t') K_{1m}(t') dt' + \int_0^L B_m(t, t') K_{2m}(t') dt' \quad (15)$$

$$\frac{1}{2} K_{2m}(t) = K_{2m}^{inc}(t) + \int_0^L C_m(t, t') K_{1m}(t') dt' + \int_0^L D_m(t, t') K_{2m}(t') dt'$$



$$\frac{1}{2} K'_{1m}(t) = K'_{2m}{}^{inc}(t) + \int_0^L A_m(t,t') K'_{1m}(t') dt' + \int_0^L B_m(t,t') K'_{2m}(t') dt' \quad (16)$$

$$\frac{1}{2} K'_{2m}(t) = K'_{2m}{}^{inc}(t) + \int_0^L C_m(t,t') K'_{1m}(t') dt' + \int_0^L D_m(t,t') K'_{2m}(t') dt'$$

where

$$A_m(t,t') = a_1(t,t') \int_0^{2\pi} \cos \theta \cos m\theta f(R) d\theta + a_2(t,t') \int_0^{2\pi} \cos m\theta f(R) d\theta$$

$$B_m(t,t') = b(t,t') \int_0^{2\pi} \sin \theta \sin m\theta f(R) d\theta$$

$$C_m(t,t') = -c(t,t') \int_0^{2\pi} \sin \theta \sin m\theta f(R) d\theta$$

$$D_m(t,t') = d_1(t,t') \int_0^{2\pi} \cos \theta \cos m\theta f(R) d\theta + d_2(t,t') \int_0^{2\pi} \cos m\theta f(R) d\theta$$

$$a_1(t,t') = (z' - z) \sin v' - \rho' \cos v'$$

$$a_2(t,t') = \rho \cos v'$$

$$b(t,t') = -(z' - z)$$

$$c(t,t') = \rho \sin v' \cos v - \rho' \sin v \cos v' + (z' - z) \sin v \sin v'$$

$$d_1(t,t') = (z' - z) \sin v + \rho \cos v$$

$$d_2(t,t') = -\rho' \cos v$$

The variables  $t$  and  $t'$  represent the arclength measured from the bottom of our body (see Figs. 1a and 1b) and we denote the total arclength of our body by  $L$ . We thus see that the  $K$  components corresponding to the two different orthogonal polarizations (parallel and perpendicular) of the incident plane wave are decoupled and can be treated separately. The minus sign introduced in (13)

allowed for the identical form between (15) and (16). In what follows we integrate numerically (15) and the same procedure will apply for (16).

We will rewrite (15) as a system of linear algebraic equations. We will divide the body in parallel zones and calculate the current densities at the center of a zone. The length of the  $n^{\text{th}}$  zone along the surface of the body ( $\hat{t}$  direction) is  $2h_n$  and we also introduce a continuous coordinate  $u$  along the direction of  $\hat{t}$ :

$$z = z_p, \rho = \rho_p \quad (p = 1 \dots N)$$

$$v = v_p, v' = v_n \quad (n = 1 \dots N)$$

$$z' = z_n + u \cos v_n$$

$$\rho' = \rho_n + u \sin v_n$$

We can now cast (15) into the following form

$$\frac{1}{2} K_{1m}(t_p) = K_{1m}^{\text{inc}}(t_p) + \sum_{n=1}^N [A_m(t_p, t_n) K_{1m}(t_n) + B_m(t_p, t_n) K_{2m}(t_n)] \quad (17)$$

$$\frac{1}{2} K_{2m}(t_p) = K_{2m}^{\text{inc}}(t_p) + \sum_{n=1}^N [C_m(t_p, t_n) K_{1m}(t_n) + D_m(t_p, t_n) K_{2m}(t_n)]$$

where

$$A_m(t_p, t_n) = \int_{-h_n}^{h_n} \int_0^\pi \{ [(z_n - z_p) \sin v_n - \rho_n \cos v_n] \cos \theta + \rho_p \cos v_n \} \cos m\theta \\ \times \frac{1-ikR}{2\pi R^3} e^{ikR(\rho_n + u \sin v_n)} d\theta du$$

$$B_m(t_p, t_n) = - \int_{-h_n}^{h_n} \int_0^\pi \{ [u \cos v_n + (z_n - z_p)] \sin \theta \sin m\theta \} \\ \times \frac{1-ikR}{2\pi R^3} e^{ikR(\rho_n + u \sin v_n)} d\theta du$$

$$C_m(t_p, t_n) = - \int_{-h_n}^{h_n} \int_0^\pi \{ [\rho_p \cos v_p + (z_n - z_p) \sin v_p] \sin v_n - \rho_n \sin v_p \cos v_n \} \\ \sin \theta \sin m\theta \times (\rho_n + u \sin v_n) \frac{1-ikR}{2\pi R^3} d\theta du$$

$$D_m(t_p, t_n) = \int_{-h_n}^{h_n} \int_0^\pi \{ [\rho_p \cos v_p + (u \cos v_n + z_n - z_p) \sin v_p] \cos \theta \\ - (\rho_n + u \sin v_n) \cos v_p \} \cos m\theta (\rho_n + u \sin v_n) \frac{1-ikR}{2\pi R^3} e^{ikR} d\theta du,$$

and

$$R^2 = u^2 + 2u[(z_n - z_p) \cos v_n + \rho_n \sin v_n] + (z_n - z_p)^2 \\ + \rho_p^2 + \rho_n^2 - 2\rho_p[\rho_n + u \sin v_n] \cos \theta$$

When  $n = p$  the integrands become singular at  $u = 0$ ,  $\theta = 0$  and one needs to apply special care to handle the numerical integration. However, we can rewrite the integrands in a way that allows us to subtract out the singularity and perform part of the integration explicitly. To that effect we rewrite  $(1-ikR/R^3)e^{ikR}$  as follows

$$\frac{1-ikR}{R^3} e^{ikR} = \frac{(1-ikR)e^{ikR} - (1+\frac{1}{2}k^2 R^2) + (1+\frac{1}{2}k^2 R^2)}{R^3} \\ = g(u, \theta) + \frac{1+\frac{1}{2}k^2 R^2}{R^3}$$

where

$$g(u, \theta) = \frac{(1-ikR)e^{ikR} - (1+\frac{1}{2}k^2 R^2)}{R^3}$$

and

$$R^2 = u^2 + 2\rho_n(1 - \cos \theta)(\rho_n + u \sin v_n)$$

The u-integrations containing  $g(u, \theta)$  have nonsingular integrands and the rest of the u-integrations can be performed explicitly. The results are

$$\begin{aligned}
 A_n(t_n, t_n) &= \frac{\rho_n \cos v_n}{2\pi} \int_0^\pi \left\{ \int_{-h_n}^{h_n} g(u, \theta) (\rho_n + u \sin v_n) du \right. \\
 &\quad + \rho_n \int_{-h_n}^{h_n} \frac{du}{R^3} + \frac{1}{2} k^2 \rho_n \int_{-h_n}^{h_n} \frac{du}{R} + \sin v_n \int_{-h_n}^{h_n} \frac{u}{R^3} du \\
 &\quad \left. + \frac{1}{2} k^2 \sin v_n \int_{-h_n}^{h_n} \frac{u}{R} du \right\} (1 - \cos \theta) \cos m\theta d\theta \\
 &= \frac{\cos v_n}{2\pi} \int_0^\pi \left\{ \frac{1}{2 - \sin^2 v_n (1 - \cos \theta)} \left[ \frac{h_n}{\rho_n} \left( \frac{1}{R_o^+} + \frac{1}{R_o^-} \right) \right. \right. \\
 &\quad \left. \left. + \sin v_n (1 - \cos \theta) \left( \frac{1}{R_o^+} - \frac{1}{R_o^-} \right) \right] \right. \\
 &\quad + \left[ K_1(\theta) - \frac{\sin v_n}{2 - \sin^2 v_n (1 - \cos \theta)} \left[ \frac{h_n}{\rho_n} \sin v_n \left( \frac{1}{R_o^+} + \frac{1}{R_o^-} \right) + 2 \left( \frac{1}{R_o^+} - \frac{1}{R_o^-} \right) \right] \right. \\
 &\quad \left. + \frac{1}{2} k^2 \rho_n^2 \left[ \sin v_n (R_o^+ - R_o^-) \right. \right. \\
 &\quad \left. \left. + [1 - \sin^2 v_n (1 - \cos \theta)] L(\theta) \right] \right\} (1 - \cos \theta) \cos m\theta d\theta
 \end{aligned}$$

$$\begin{aligned}
B_m(t_n, t_n) &= -\frac{\cos v_n}{2\pi} \int_0^\pi \left\{ \int_{-h_n}^{h_n} g(u, \theta) (\rho_n + u \sin v_n) u du + \rho_n \int_{-h_n}^{h_n} \frac{udu}{R^3} \right. \\
&\quad + \frac{1}{2} k^2 \rho_n \int_{-h_n}^{h_n} \frac{udu}{R} + \sin v_n \int_{-h_n}^{h_n} \frac{u^2 du}{R^3} \\
&\quad \left. + \frac{1}{2} k^2 \sin v_n \int_{-h_n}^{h_n} \frac{u^2 du}{R} \right\} \sin \theta \sin m\theta d\theta \\
&= -\frac{\cos v_n}{2\pi} \int_0^\pi \left\{ K_2(\theta) - \frac{1}{2 \sin^2 v_n (1 - \cos \theta)} \left[ \frac{h_n}{\rho_n} \sin v_n \left( \frac{1}{R_o^+} + \frac{1}{R_o^-} \right) \right. \right. \\
&\quad \left. \left. + 2 \left( \frac{1}{R_o^+} - \frac{1}{R_o^-} \right) \right] + \frac{2 \sin v_n}{2 \sin^2 v_n (1 - \cos \theta)} \left[ \sin^2 v_n (1 - \cos \theta) - 1 \right] \left( \frac{1}{R_o^+} + \frac{1}{R_o^-} \right) \frac{h_n}{\rho_n} \right. \\
&\quad \left. + \sin v_n (1 - \cos \theta) \left( \frac{1}{R_o^+} - \frac{1}{R_o^-} \right) \right] + \sin v_n L(\theta) \\
&\quad + \frac{1}{2} k^2 \rho_n^2 \left[ \frac{1}{2} \frac{h_n}{\rho_n} \sin v_n (R_o^+ + R_o^-) + \left[ 1 - \frac{3}{2} \sin^2 v_n (1 - \cos \theta) \right] (R_o^+ - R_o^-) \right. \\
&\quad \left. + \sin v_n (1 - \cos \theta) \left[ \frac{3}{2} \sin^2 v_n (1 - \cos \theta) - 2 \right] L(\theta) \right\} \sin \theta \sin m\theta d\theta
\end{aligned}$$

$$C_m(t_n, t_n) = 0$$

$$\begin{aligned}
D_m(t_n, t_n) &= -\frac{\cos v_n}{2\pi} \int_0^\pi \left\{ \int_{-h_n}^{h_n} g(u, \theta) (\rho_n + u \sin v_n)^2 du + \rho_n^2 \int_{-h_n}^{h_n} \frac{du}{R^3} \right. \\
&\quad + \frac{1}{2} k^2 \rho_n^2 \int_{-h_n}^{h_n} \frac{du}{R} + 2\rho_n \sin v_n \int_{-h_n}^{h_n} \frac{udu}{R^3} + k^2 \rho_n \sin v_n \int_{-h_n}^{h_n} \frac{udu}{R} \\
&\quad \left. + \sin^2 v_n \int_{-h_n}^{h_n} \frac{u^2 du}{R^3} + \frac{1}{2} k^2 \sin^2 v_n \int_{-h_n}^{h_n} \frac{u^2 du}{R} \right\} \times (1 - \cos \theta) \cos m\theta d\theta \\
&= -\frac{\cos v_n}{2\pi} \int_0^\pi \left\{ \frac{1}{2 - \sin^2 v_n (1 - \cos \theta)} \left[ \frac{h_n}{\rho_n} \left( \frac{1}{R_o^+} + \frac{1}{R_o^-} \right) + \sin v_n (1 - \cos \theta) \left( \frac{1}{R_o^+} - \frac{1}{R_o^-} \right) \right] \right. \\
&\quad + (1 - \cos \theta) \left\{ \frac{2 \sin v_n}{2 - \sin^2 v_n (1 - \cos \theta)} \left[ \frac{h_n}{\rho_n} \sin v_n [\sin^2 v_n (1 - \cos \theta) - 2] \left( \frac{1}{R_o^+} + \frac{1}{R_o^-} \right) \right. \right. \\
&\quad \left. \left. + [\sin^2 v_n (1 - \cos \theta) - 2] \left( \frac{1}{R_o^+} - \frac{1}{R_o^-} \right) \right] + K_4(\theta) + \sin^2 v_n L(\theta) \right. \\
&\quad \left. + \frac{1}{2} k^2 \rho_n^2 \left[ \sin v_n \left[ 2 - \frac{3}{2} \sin^2 v_n (1 - \cos \theta) \right] (R_o^+ - R_o^-) \left[ 1 + \sin^2 v_n (1 - \cos \theta) \right] \right. \right. \\
&\quad \left. \left. \left[ \frac{3}{2} \sin^2 v_n (1 - \cos \theta) - 3 \right] L(\theta) + \frac{1}{2} \sin^2 v_n \frac{h_n}{\rho_n} (R_o^+ + R_o^-) \right] \right\} \cos m\theta d\theta
\end{aligned}$$

where

$$R_o^+ = \left[ \frac{h_n^2}{\rho_n^2} + 2 \left( 1 + \frac{h_n}{\rho_n} \sin v_n \right) (1 - \cos \theta) \right]^{\frac{1}{2}}$$

$$R_o^- = \left[ \frac{h_n^2}{\rho_n^2} + 2 \left( 1 - \frac{h_n}{\rho_n} \sin v_n \right) (1 - \cos \theta) \right]^{\frac{1}{2}}$$

$$L(\theta) = \ln \frac{\sin v_n (1 - \cos \theta) + (h_n / \rho_n) + R_o^+}{\sin v_n (1 - \cos \theta) - (h_n / \rho_n) + R_o^-}$$

$$K_1(\theta) = \int_{-h_n}^{h_n} g(u, \theta) (\rho_n + u \sin v_n) \rho_n du$$

$$K_2(\theta) = \int_{-h_n}^{h_n} g(u, \theta) (\rho_n + u \sin v_n) u du$$

$$K_4(\theta) = \int_{-h_n}^{h_n} g(u, \theta) (\rho_n + u \sin v_n)^2 du$$

$$g(u, \theta) = \frac{(1 - ikR) e^{ikR} - (1 + \frac{1}{2} k^2 R^2)}{R^3}$$

$$R^2 = u^2 + 2\rho_n(1 - \cos \theta)(\rho_n + u \sin v_n)$$

This completes the definition of all of the terms in (17) and reduces the problem to one of matrix inversion. Still left to be decided is the zoning on the body. The study of scattering by a metallic cylinder reported in a previous note [2] can serve as a guideline. In that study two basic requirements were determined. a) To secure sufficient numerical accuracy for the calculation of the surface current density at least 17 sample points per wavelength were chosen. b) The integral equation we use is based on the magnetic field formulation which requires that the diagonal elements of the associated matrix be the largest elements. This requirement is translated into the condition that the length of a zone should not exceed the minimum radius of the body associated with any point included in the zone. A computer code based on (17) which incorporates the associated matrix inversion has been written.

Also incorporated in the code is the capability of calculating the induced current density when the incident plane wave has an arbitrary time dependence. This is accomplished by utilizing the preceding analysis and then employing Fourier inversion techniques.

## Discussion of Results

Our primary purpose was to develop a set of equations upon which a computer code could be based. The purpose of that code is to calculate the induced surface current density that results when a perfectly conducting body of revolution is illuminated by a plane wave. The basic set of equations which accomplish this purpose are presented in (17). The analysis leading to (17) was time harmonic; however, the code is capable of calculating the induced current density for an incident plane wave having an arbitrary time dependence. This is accomplished by employing Fourier inversion techniques.

In this note we used the code to calculate the total current induced on a perfectly conducting cylinder of finite length when the incident plane wave had both a time harmonic and a step function time dependence. In these calculations we set  $\theta_p$  equal to zero so that the axis of the cylinder, the wave normal, and the electric field all lie in the same plane. All of our results are for the case where the length of the cylinder is ten times its diameter. The points of interest on the cylinder as well as a description of the incident plane wave are depicted in figure 3. In figures 5 through 9 we plot the magnitude of the induced current versus frequency. Figure 5 corresponds to the incident angle,  $\theta_i$ , equal to  $75^\circ$  while figure 9 corresponds to  $\theta_i$  equal to  $15^\circ$ . The intermediate figures correspond to the values  $\theta_i$  spaced at  $15^\circ$  intervals. Figure 4 is taken from a previous note [2] and corresponds to normal incidence,  $\theta_i = 90^\circ$ . In figures 5 through 9 we plot the current that exists at three different points on the cylinder, at the center and at the two points halfway between the center and each end. In these plots the current has the largest peak value at the center of the cylinder. In figures 11 through 15 we plot the current at the same three points on the cylinder versus time. The origin of the time scale for each point on the cylinder is defined so that  $t$  equals zero when the incident plane wave first strikes that point. Each figure corresponds to a different value of  $\theta_i$ , again ranging from  $75^\circ$  to  $15^\circ$  in  $15^\circ$  intervals. Figure 10 is again taken from a previous note [2]. The induced current in this figure has the opposite direction from the currents calculated in this note because the incident electric field considered in that note has the opposite direction from the one considered in this note. All of these time dependent



plots correspond to the incident field having a step function time dependence. It is interesting to note that the maximum peak current no longer occurs at the center of the cylinder. In figures 10 and 11 the largest peak occurs at the center of the cylinder, while in figures 12 through 15, the peak occurs halfway between the center and the upper end of the cylinder. A physical explanation for this can be given. First, we note that the current at a particular point will continually increase until it experiences the subtractive current reflected from the ends of the cylinder. For  $\theta_i$  equal to  $90^\circ$  and  $75^\circ$  the center point will feel the effect of an end after a longer time than either of the other two points. For the remaining angles the upper point feels the effect of an end after a longer time than the other points and it experiences the largest peak current.

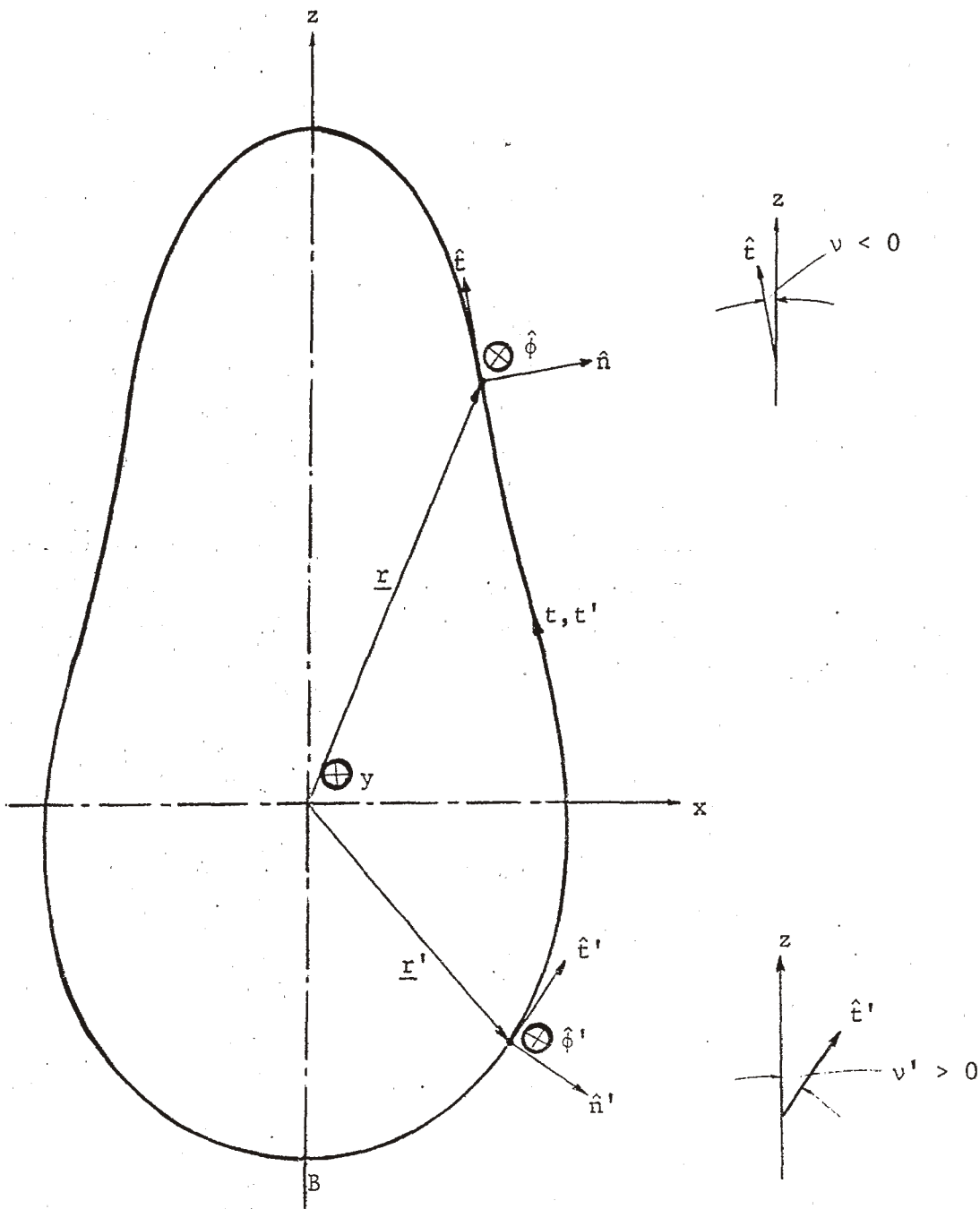


Figure 1a. Local Orthogonal Curvilinear Coordinate Systems.  
 $t, t'$  are the coordinate variables used to represent  
the arclength measured from the bottom point B.

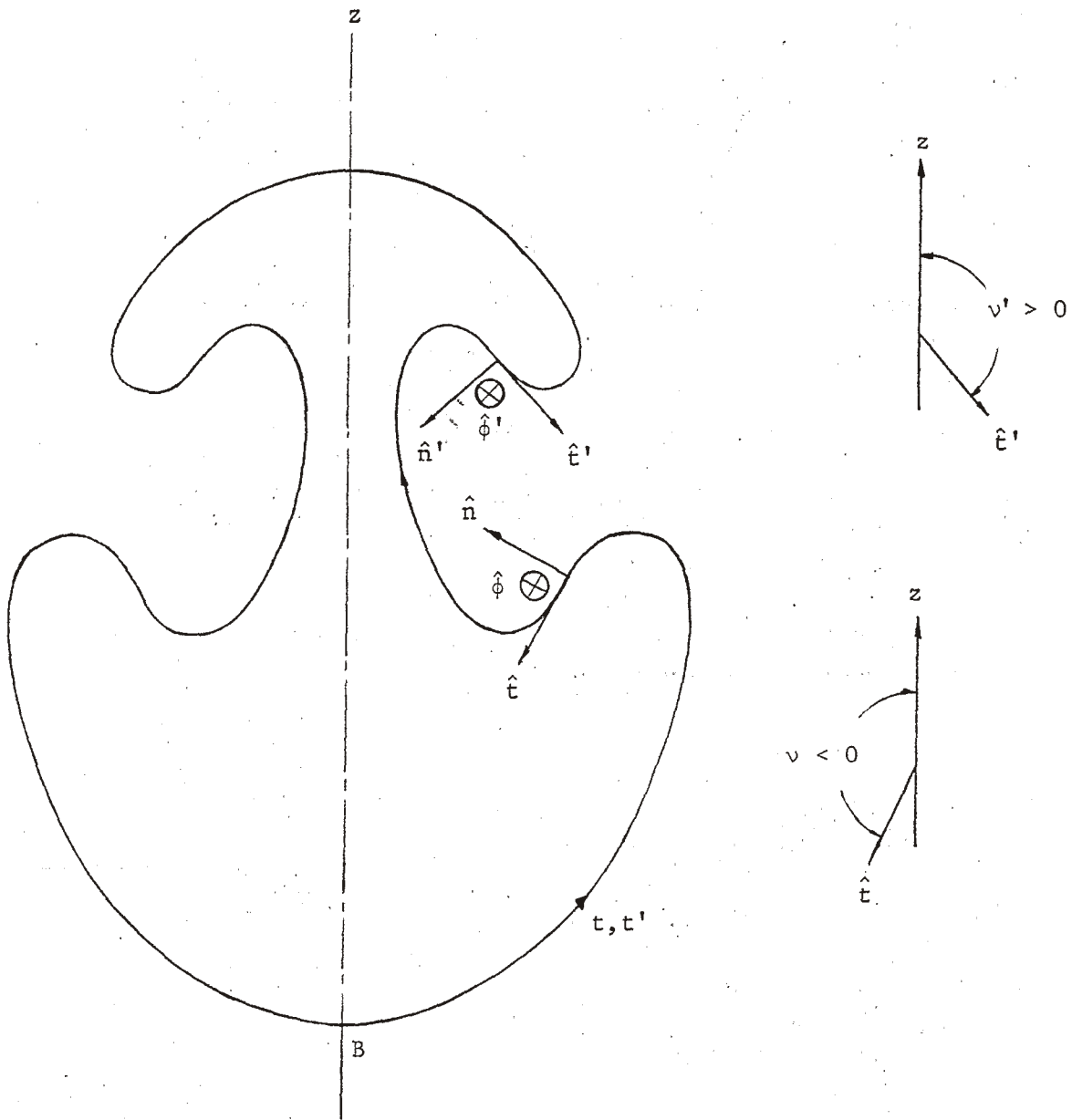


Figure 1b. Local Orthogonal Curvilinear Coordinate Systems.  $t, t'$  are the coordinate variables used to represent the arclength measured from the bottom point  $B$ .

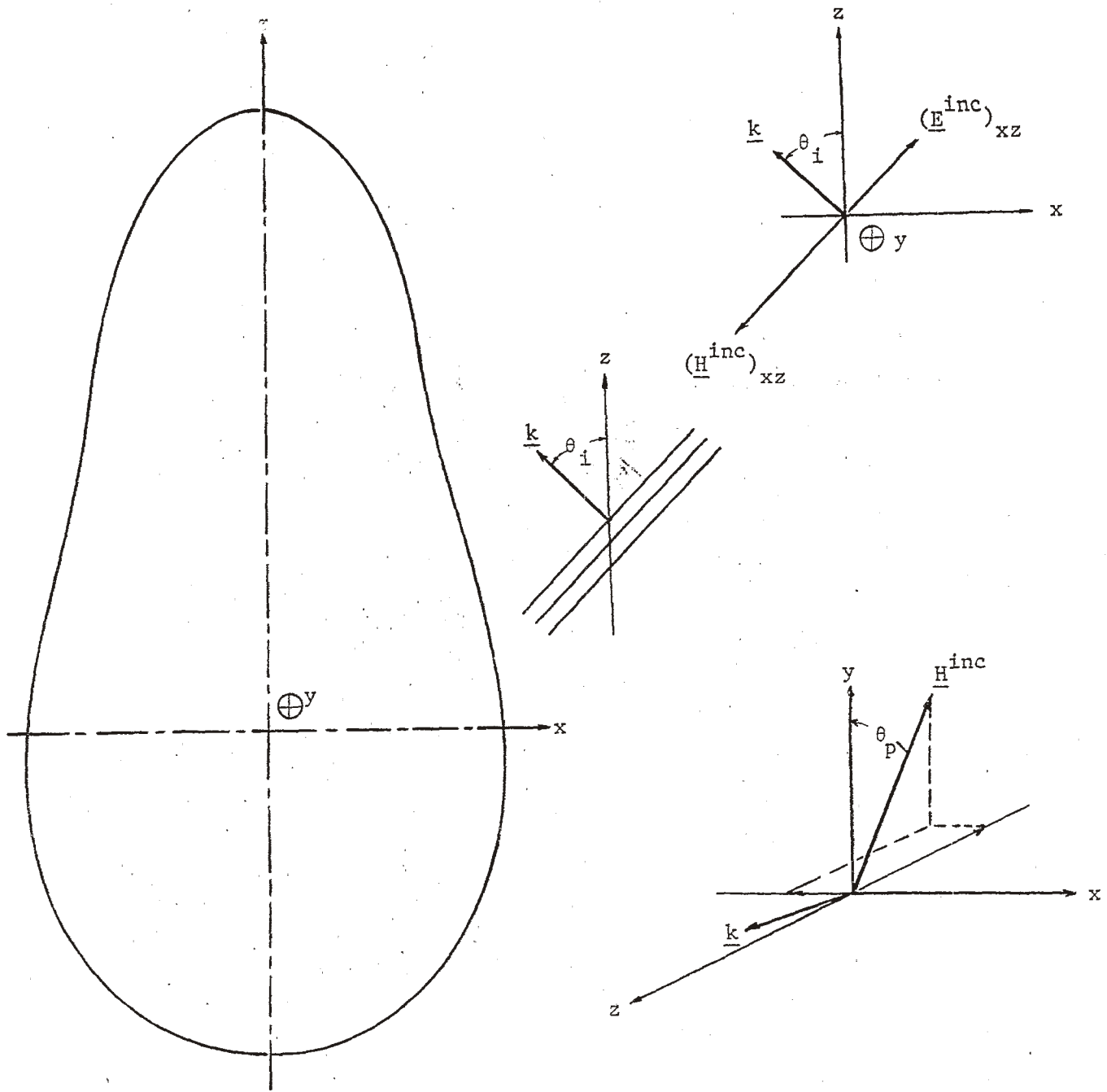


Figure 2. Incident Plane Wave Description.

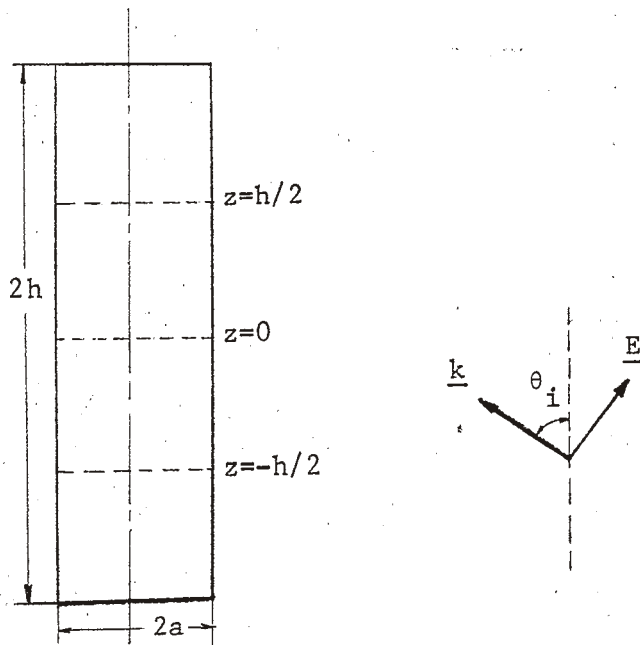


Figure 3. Geometry of Cylinder and Incident Plane Wave

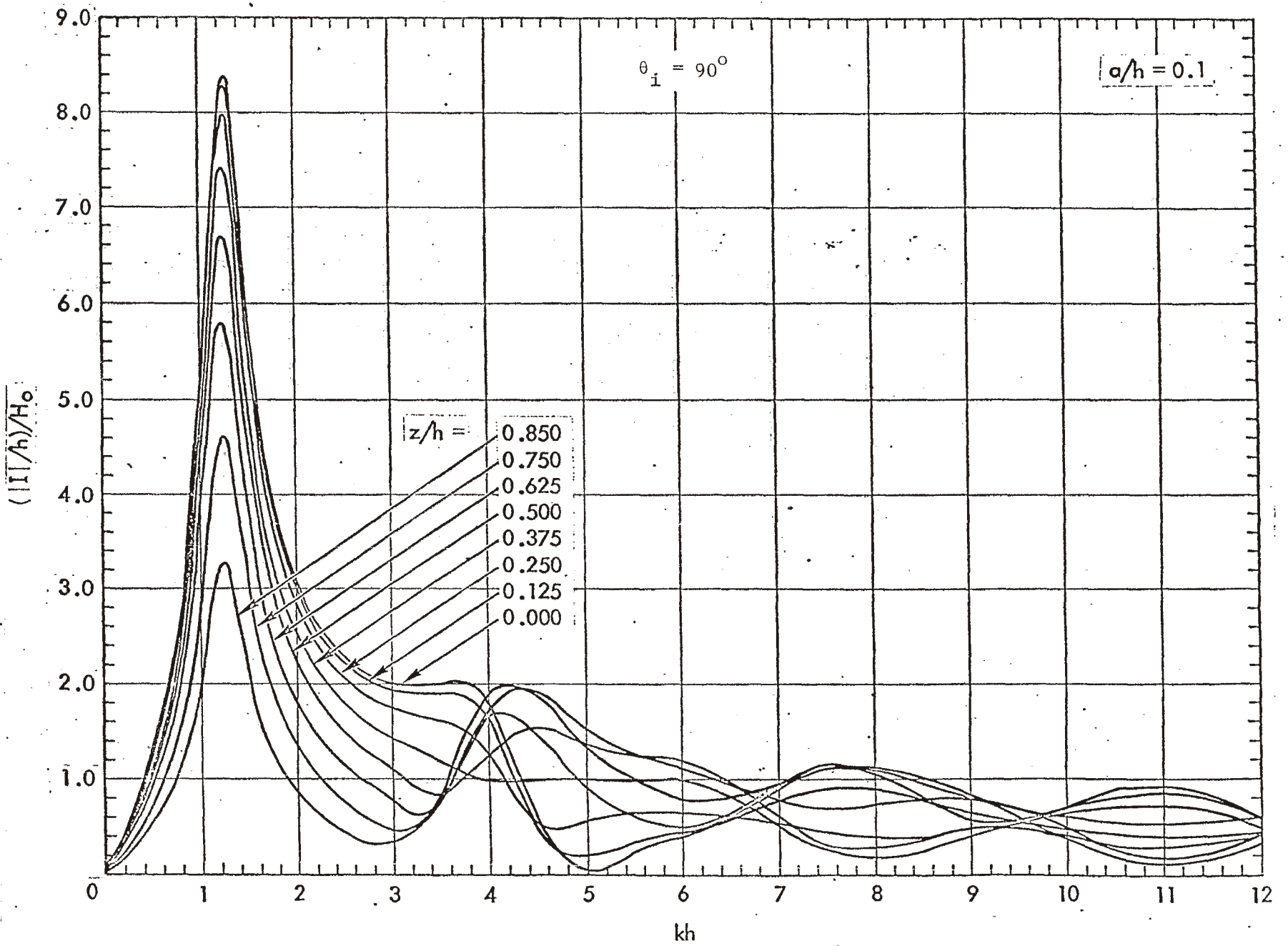


Figure 4. Magnitude of the Current on a Cylinder Scattering a Plane Wave versus  $kh$

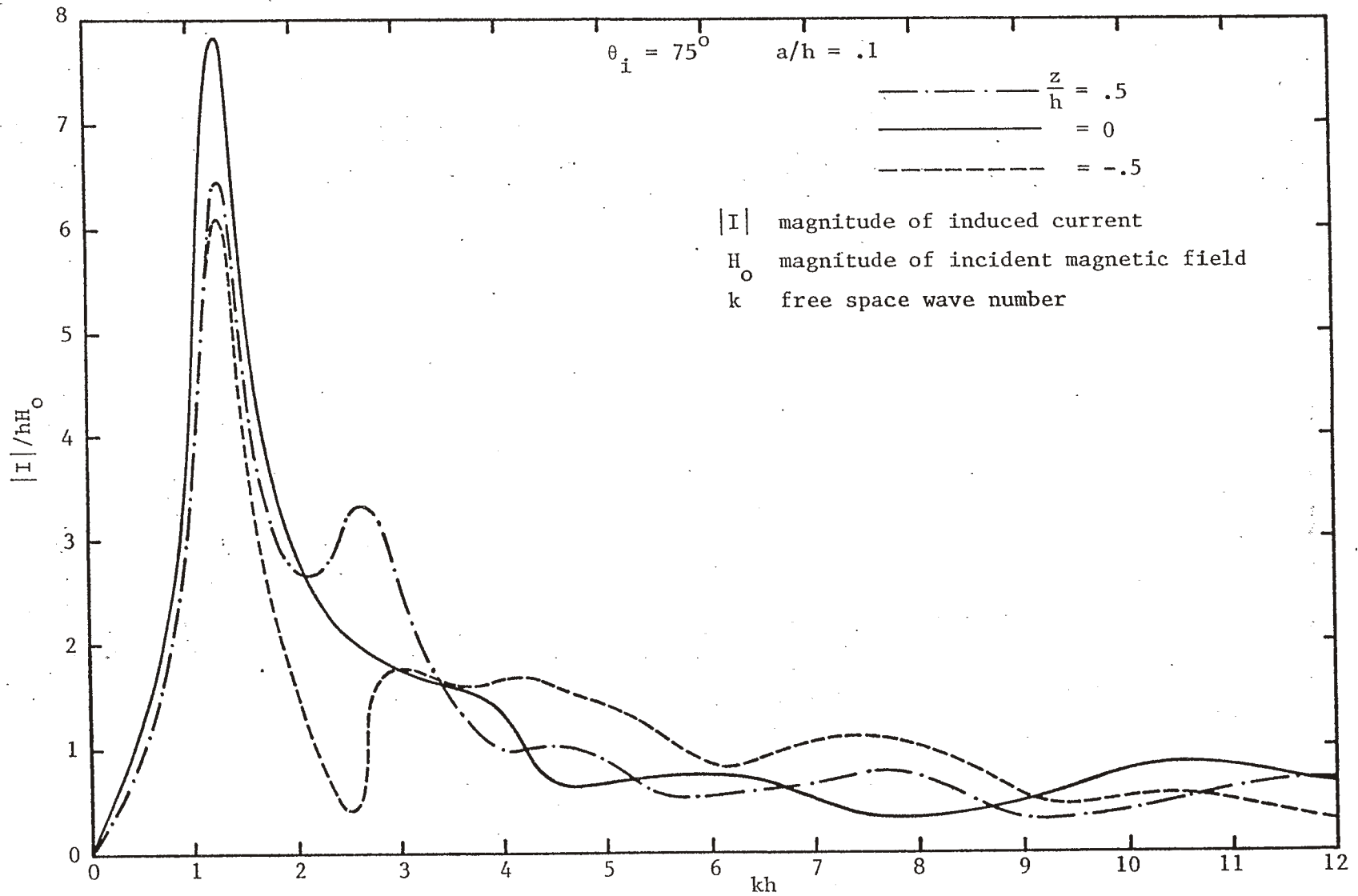


Figure 5. Magnitude of the Current on a Cylinder Scattering a Plane Wave versus  $kh$

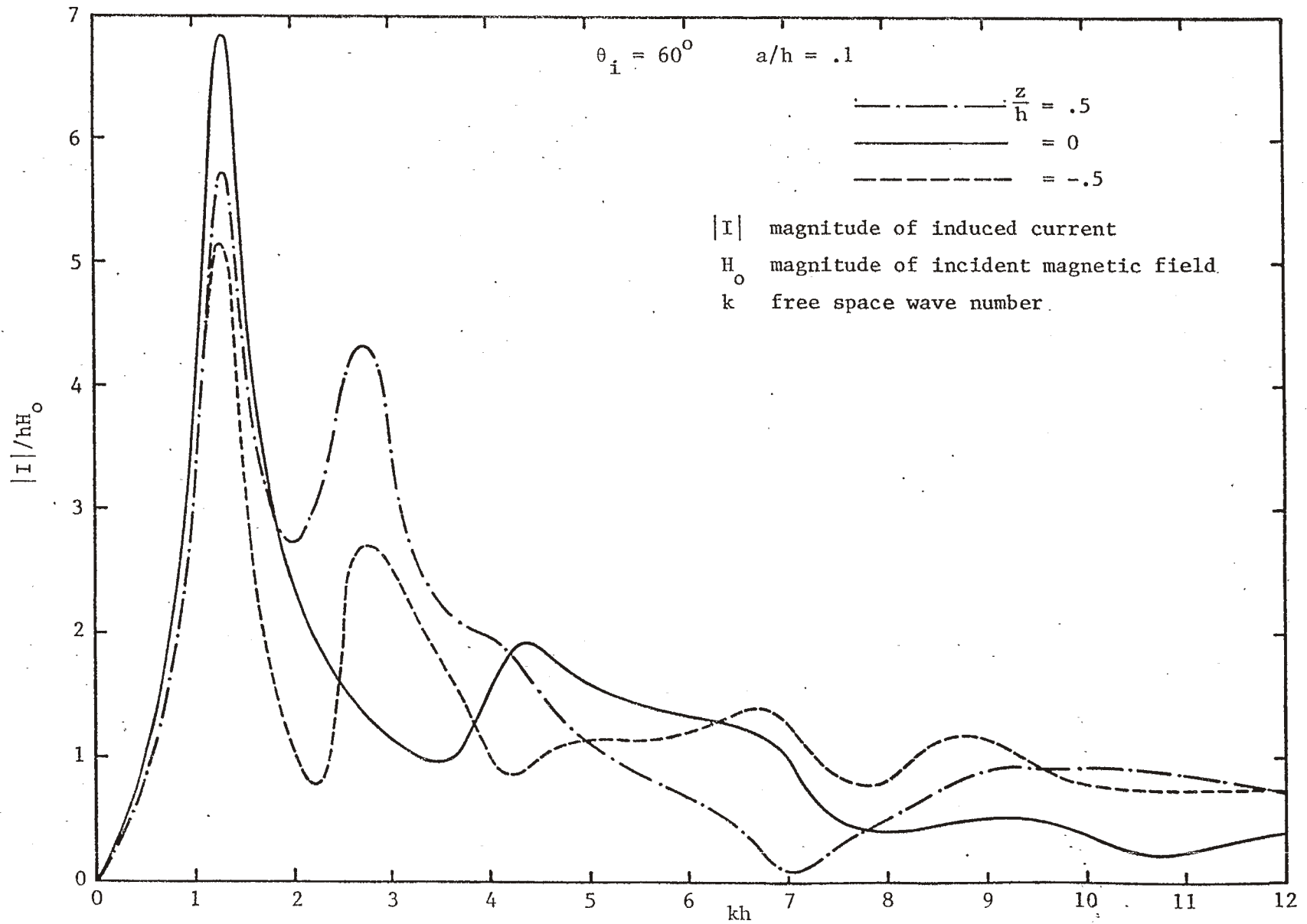


Figure 6. Magnitude of the Current on a Cylinder Scattering a Plane Wave versus  $kh$



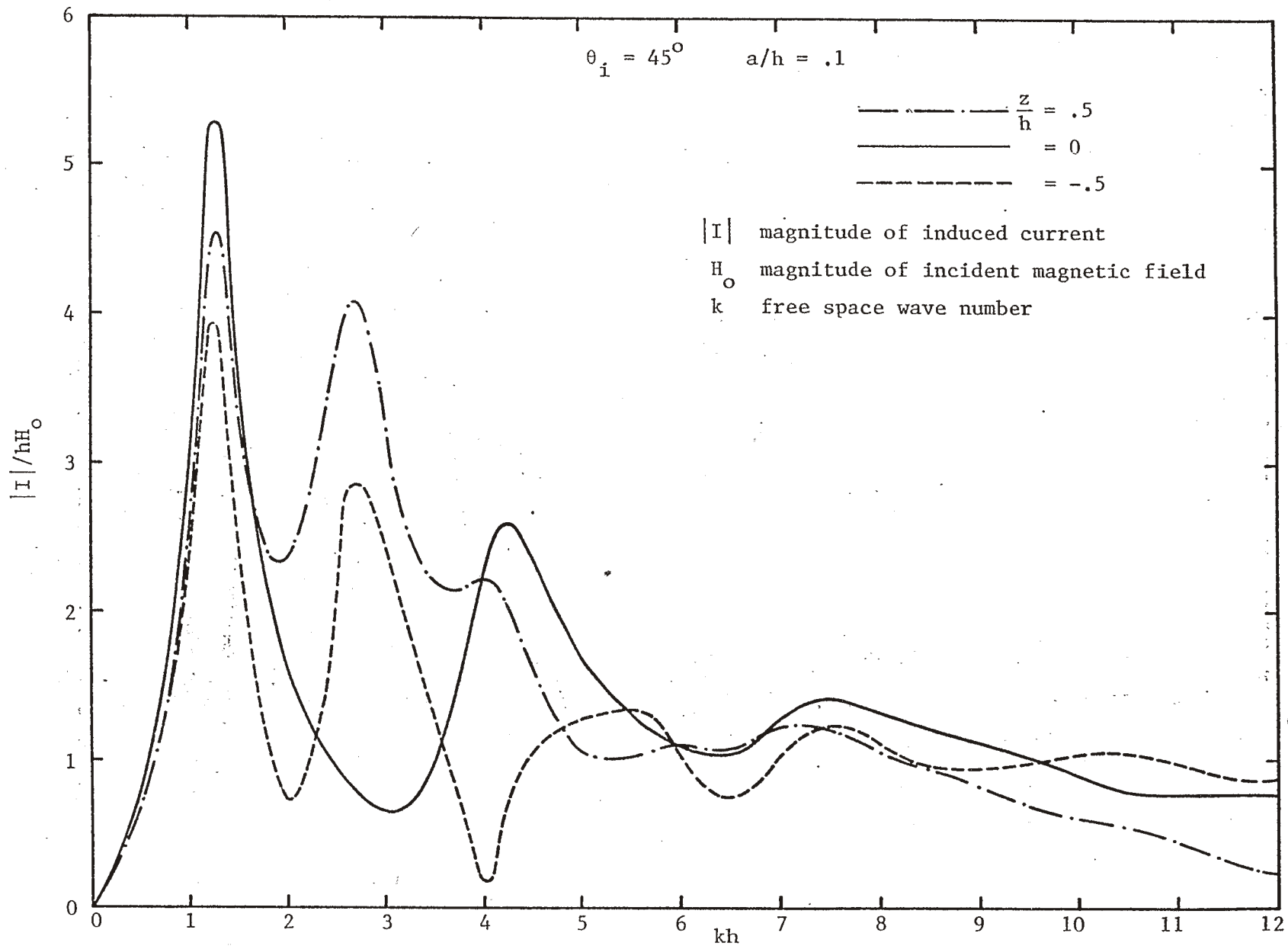


Figure 7. Magnitude of the Current on a Cylinder Scattering a Plane Wave versus  $kh$

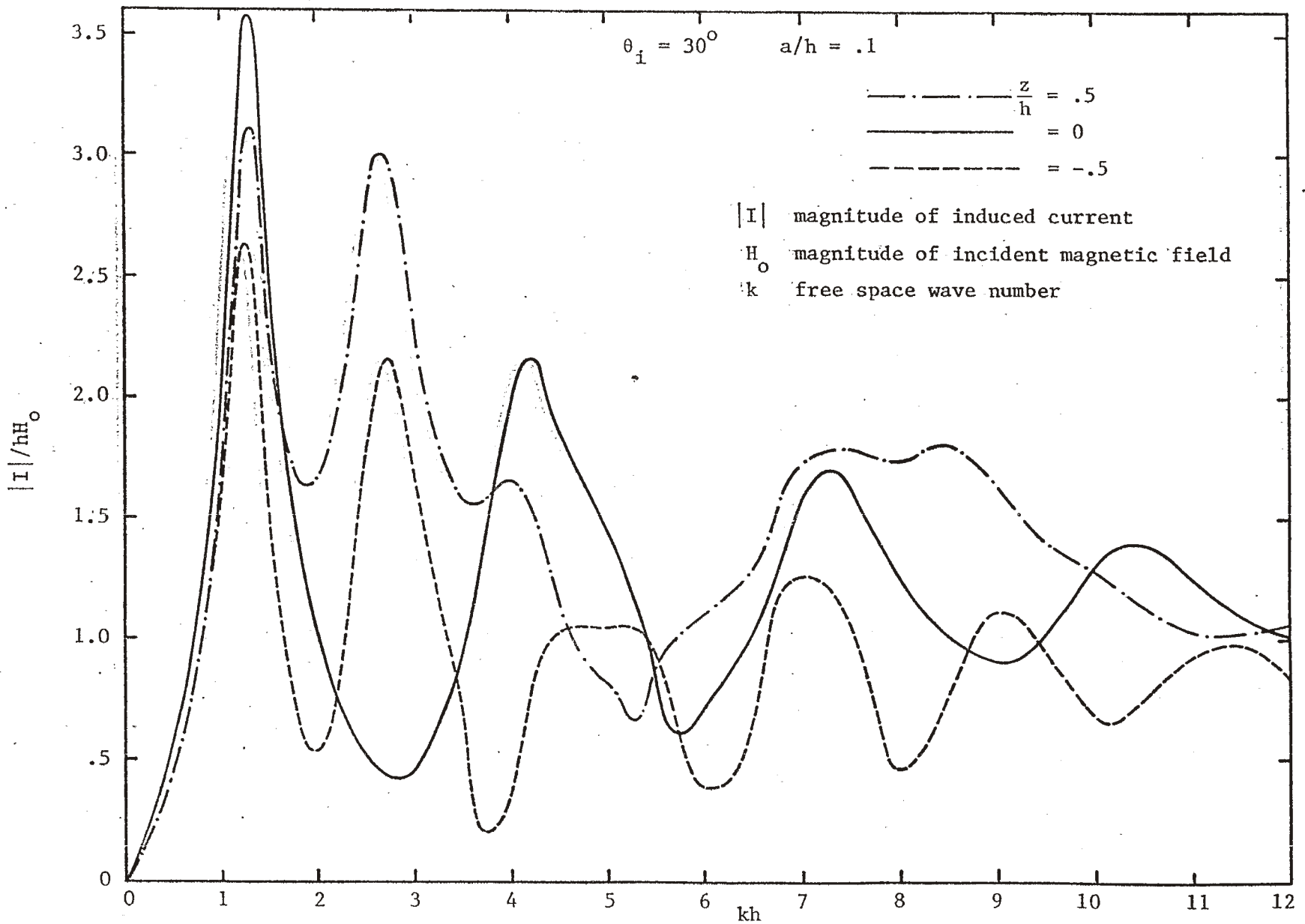


Figure 8. Magnitude of the Current on a Cylinder Scattering a Plane Wave versus  $kh$

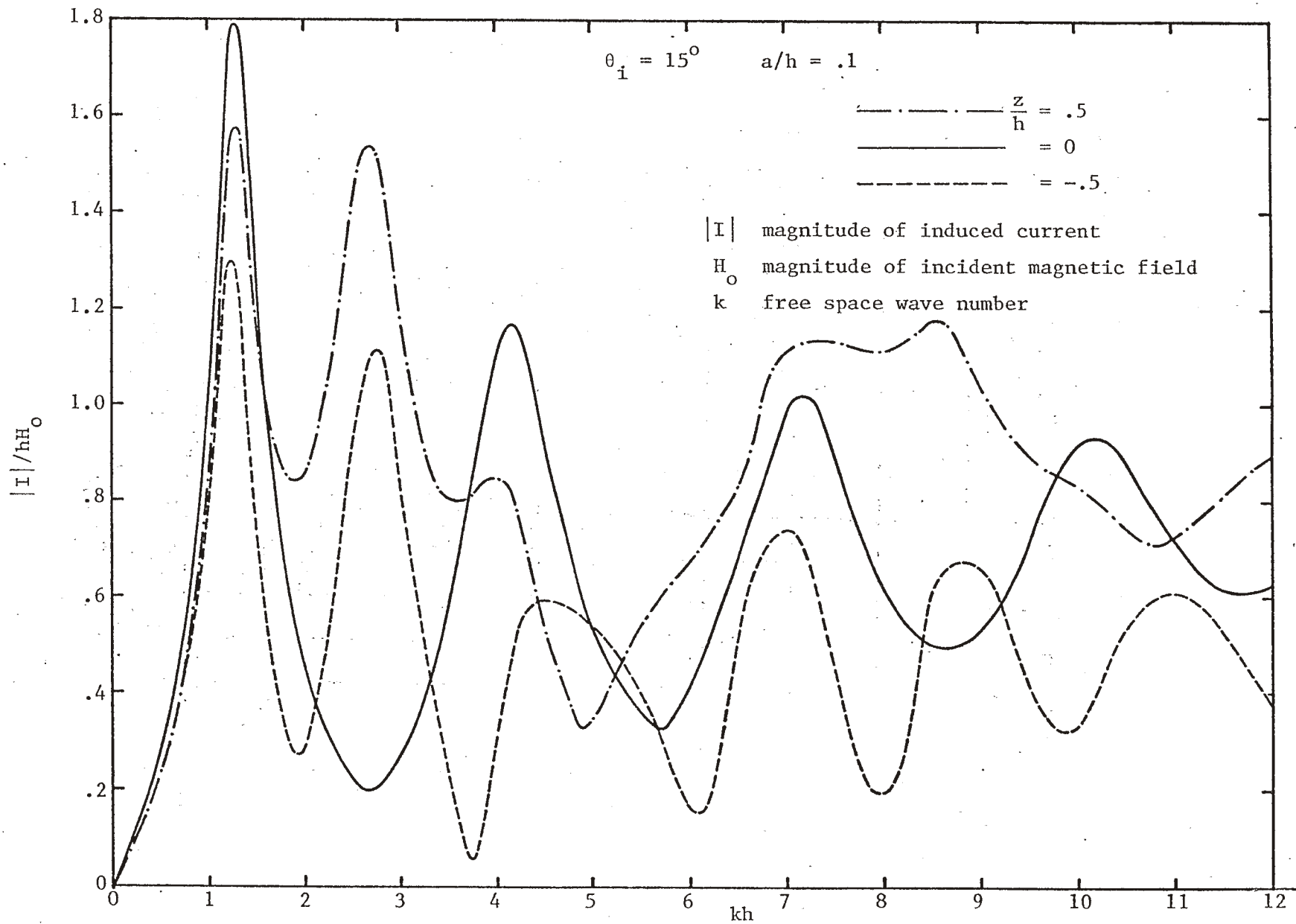


Figure 9. Magnitude of the Current on a Cylinder Scattering a Plane Wave versus  $kh$

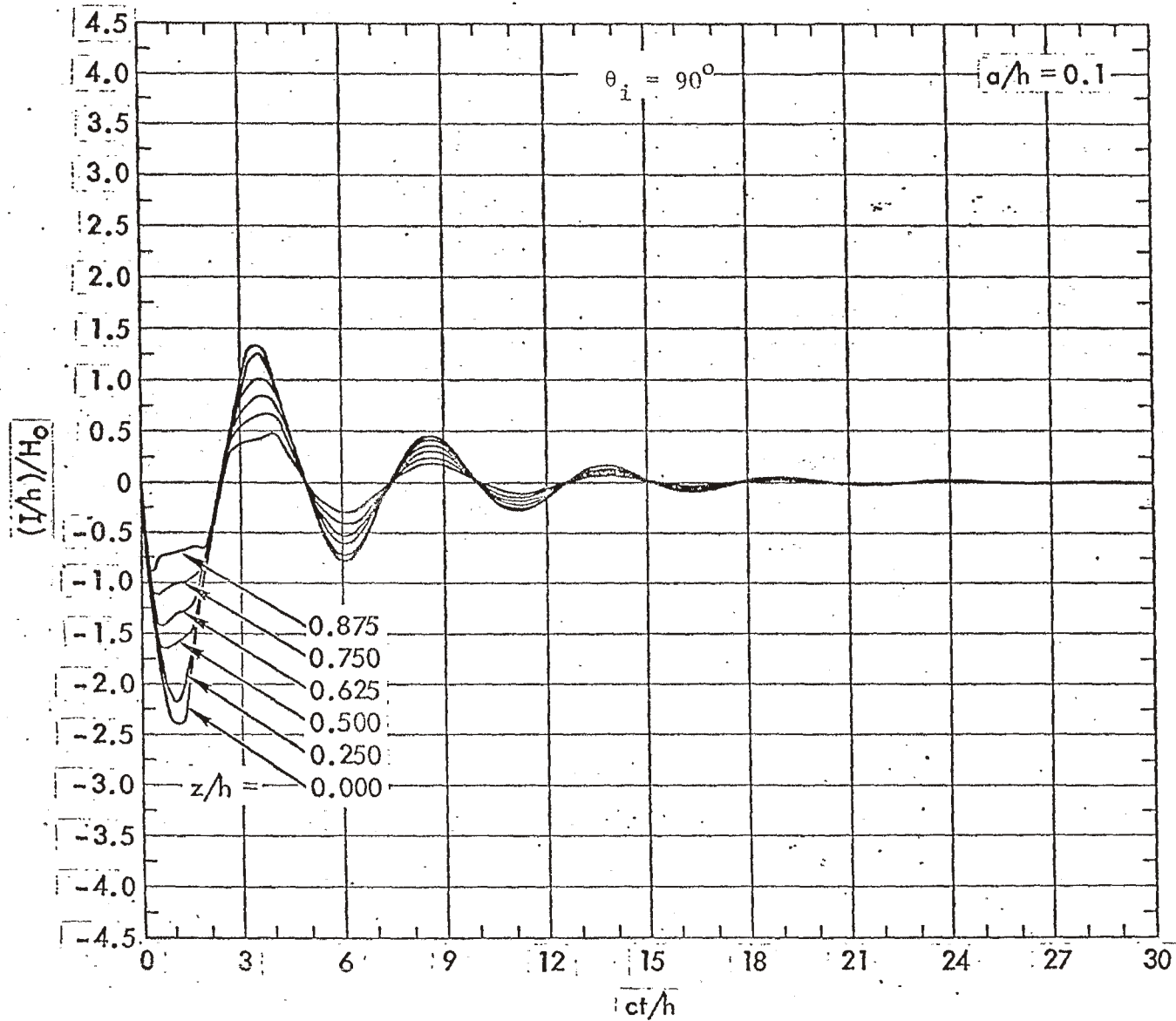


Figure 10. Current on a Cylinder Induced by a Unit Step of Magnetic Field versus  $ct/h$ .

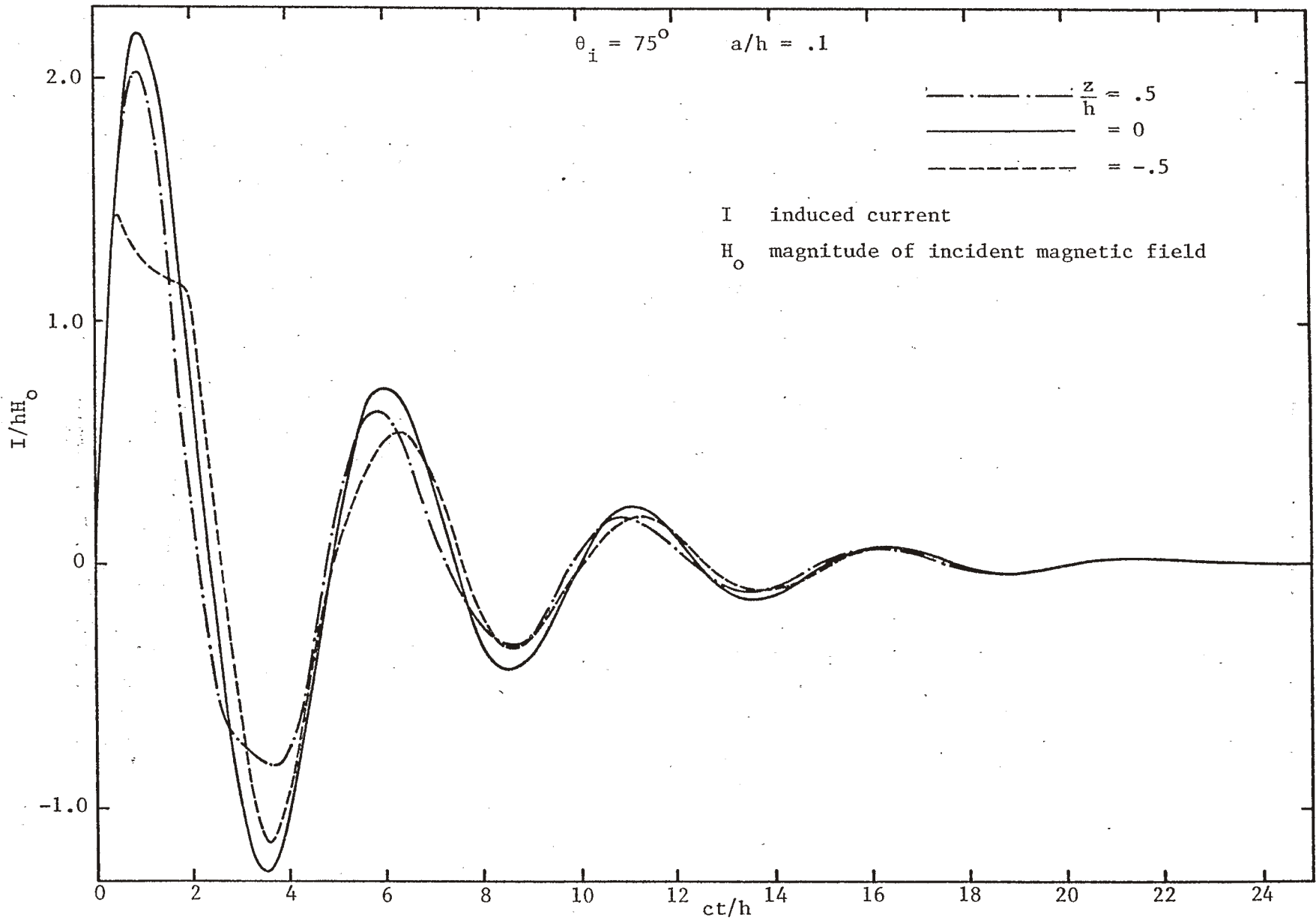


Figure 11. Current on a Cylinder Induced by a Unit Step of Magnetic Field versus  $ct/h$

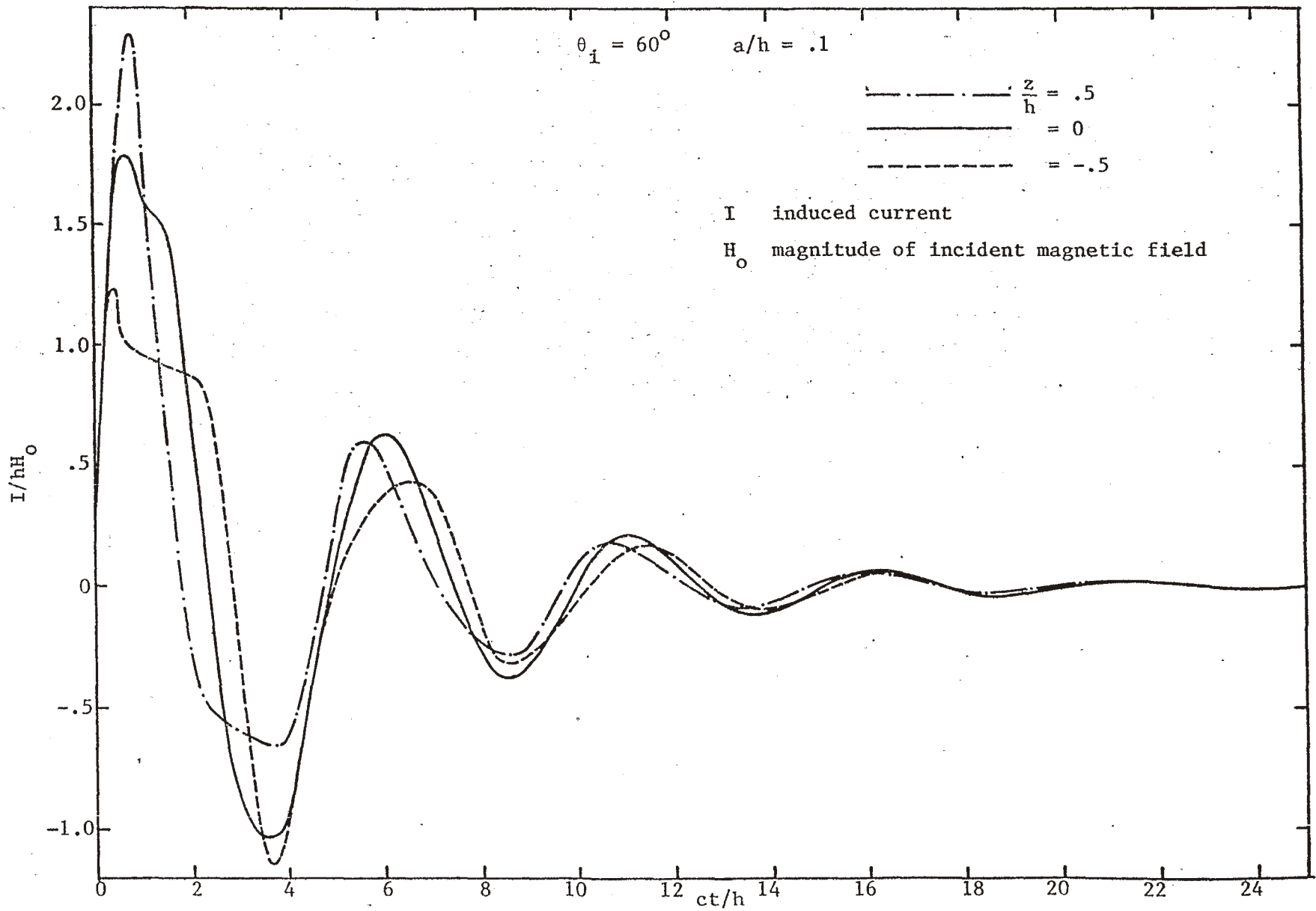


Figure 12. Current on a Cylinder Induced by a Unit Step of Magnetic Field versus  $ct/h$

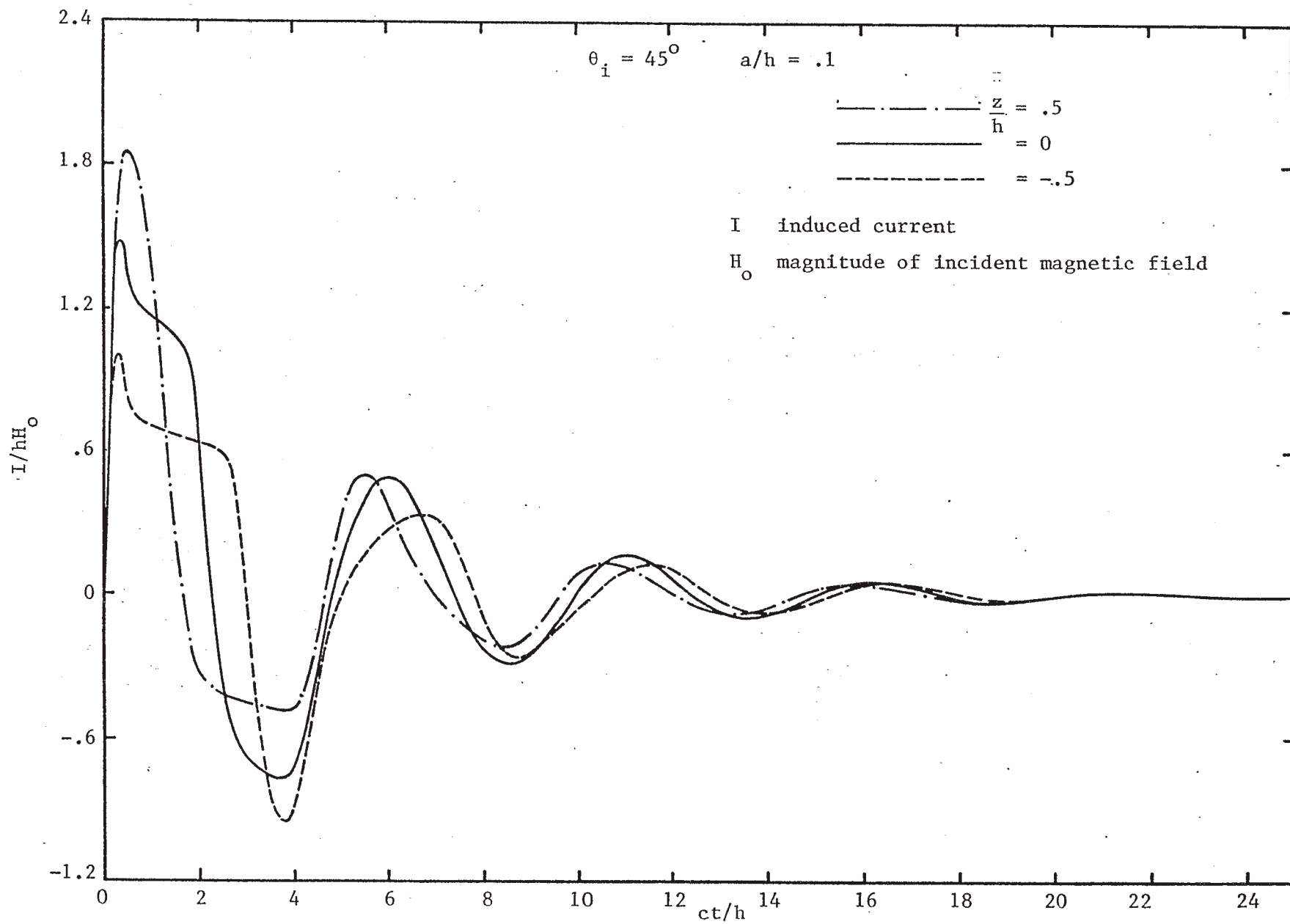


Figure 13. Current on a Cylinder Induced by a Unit Step of Magnetic Field versus  $ct/h$

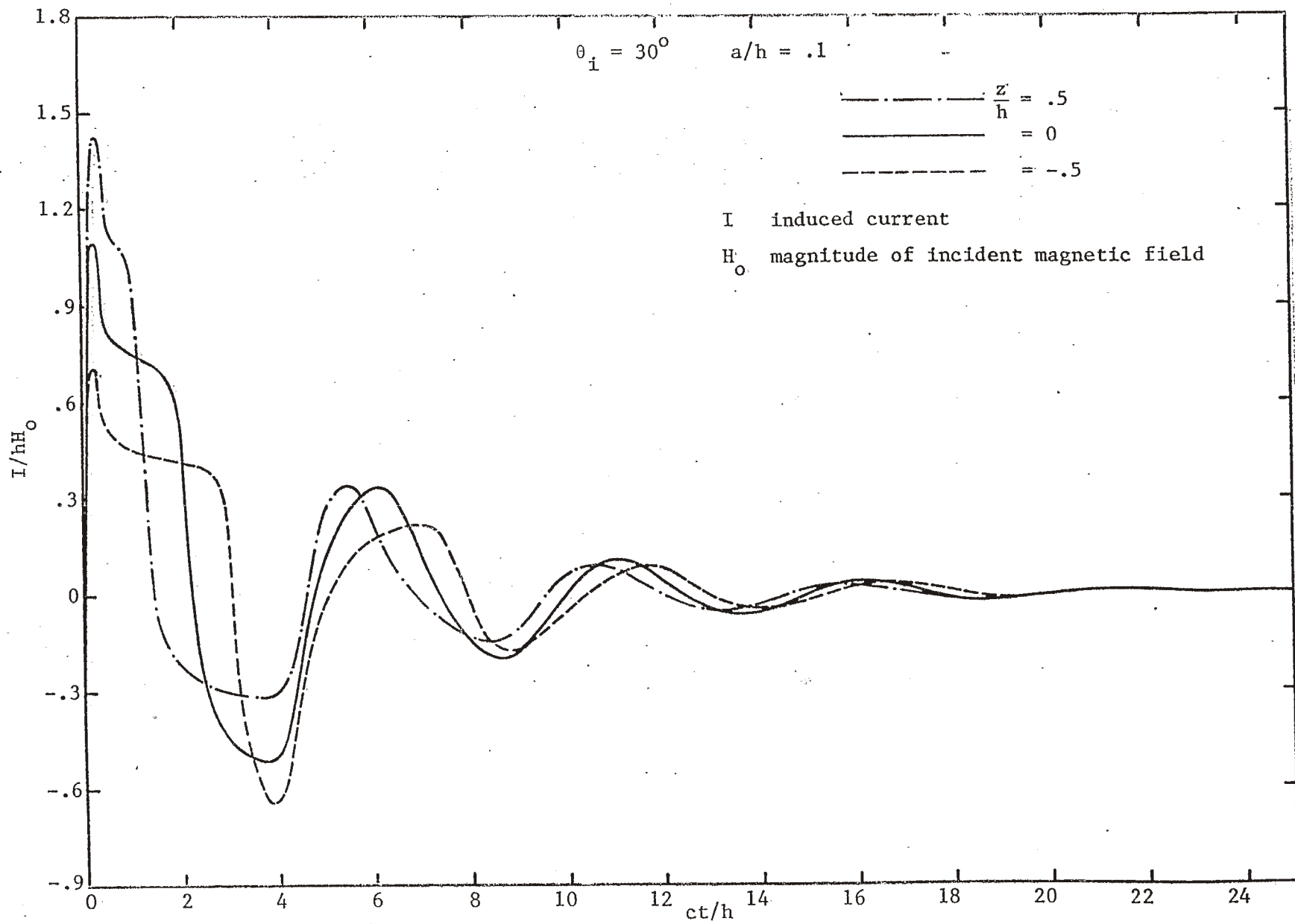


Figure 14. Current on a Cylinder Induced by a Unit Step of Magnetic Field versus  $ct/h$



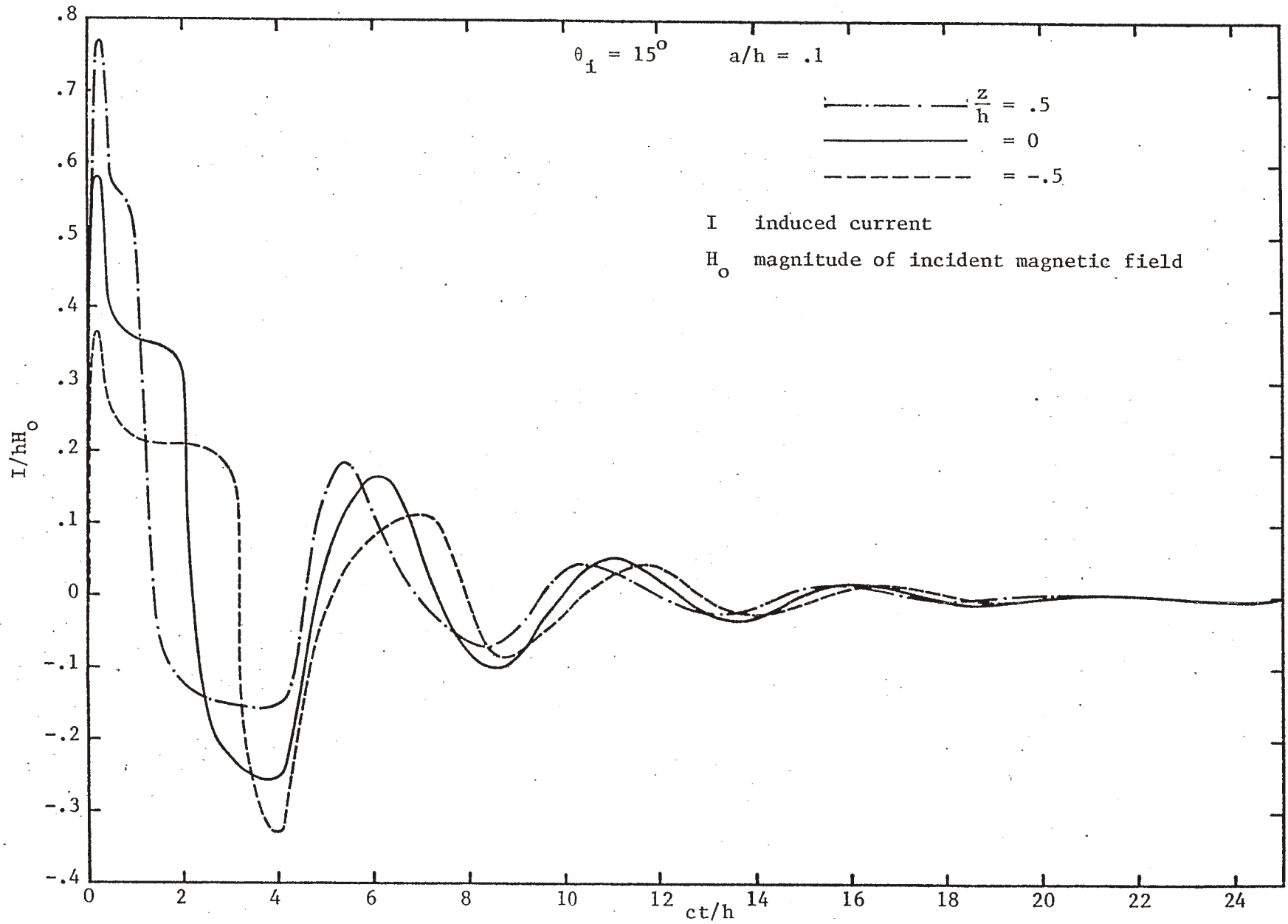


Figure 15. Current on a Cylinder Induced by a Unit Step of Magnetic Field versus  $ct/h$

### Acknowledgement

We thank Dr. C. E. Baum for suggesting this problem and Mr. R. W. Sassman whose effort in performing the numerical work made this note possible. We also thank Mrs. G. Peralta, in particular, for her help in preparing the curves.

#### References

- [1] M. G. Andreasen, "Scattering From Bodies of Revolution," IEEE Transactions on Antennas and Propagation, AP-13, p. 303, 1965.
- [2] R. W. Sassman, "The Current Induced on a Finite, Perfectly Conducting, Solid Cylinder in Free Space by an Electromagnetic Pulse," Electromagnetic Pulse Interaction Note No. 11, 1967.
- [3] G. W. Carlisle, "Integral Equation Approach for Determining Radar Cross-Section of Rotationally Symmetric Body," McDonnell Douglas Report SM-52398.